

Preparation of Membrane-Electrode Assemblies of Solid Oxide Fuel Cells by Co-Sintering of Electrodes¹

I. N. Burmistrov*, D. A. Agarkov, F. M. Tsybrov, and S. I. Bredikhin

Institute of Solid State Physics, Russian Academy of Sciences, ul. Akademika Osip'yana, Chernogolovka, Moscow oblast, 142432 Russia

*e-mail:buril@issp.ac.ru

Received July 24, 2015

Abstract—The results of the development of procedures for forming membrane-electrode assemblies (MEAs) of solid oxide fuel cells (SOFCs) by co-sintering of electrodes and electrochemical trials of MEAs were described. Plates of HionicTM material (Fuel Cell Materials, United States) with an area of $50 \times 50 \text{ mm}^2$ were used as a solid electrolyte membrane. The cathode layers were prepared from cation-deficient lanthanum-strontium manganite and the anion conductor 89 mol % ZrO_2 –10 mol % Sc_2O_3 –1 mol % CeO_2 (10Sc1CeSZ) with a soot addition for control over the microstructure. The anode layers were formed from the composite NiO/10Sc1CeSZ and by introducing rice starch as a pore-forming agent in the anode current-collecting layer. The thermal treatment mode was optimized based on thermogravimetry and scanning electron microscopy data and the results of testing the electrochemical characteristics of SOFCs to provide the formation of electrochemically active electrodes using one thermal cycle.

Keywords: solid oxide fuel cells, membrane-electrode assemblies, co-sintering, electrodes, voltage-current characteristics

DOI: 10.1134/S1023193516070053

INTRODUCTION

Solid oxide fuel cells (SOFCs) are promising power sources that convert the chemical energy of fuel into electric and thermal energy. One variant of SOFC batteries is electrolyte-supporting construction in which the solid electrolyte membrane has the largest thickness among the SOFC components and carries the main mechanical loads [1].

To increase the fraction of the electrochemically active surface of SOFC membranes limited by the design elements and the high-temperature sealant, it is necessary to increase the area of the solid-electrolyte membrane; in this case, its thickness is generally up to 150 μm . The simultaneous increase in the geometrical area and decrease in the thickness of the supporting membrane considerably limits the applicability of the method of sequential formation of electrode layers, which requires a series of high-temperature treatments at different temperatures. During the sequential formation of electrodes, mechanical stresses appear in the electrolyte [2, 3], which lead to a considerable deformation and even decomposition of the support [4, 5]. One approach to the preparation of a membrane-electrode assembly (MEA) of the electrolyte-supporting construction with a large geometrical area

is co-sintering of electrodes. This method involves the formation of a MEA in one cycle of temperature treatment when the mechanical stresses arising in the membrane during the sintering of the cathode and anode layers compensate each other [6, 7].

Previously, we presented the results of our studies on the preparation of SOFC MEAs by separate sintering of electrodes [8, 9]. The anodes were prepared from composites of NiO and a fluorite-like solid solution with a composition of 89 mol % ZrO_2 –10 mol % Sc_2O_3 –1 mol % CeO_2 (10Sc1CeSZ) with mass ratios of phases of 40 : 60 and 60 : 40; the sintering temperature was 1380°C. For the cathode layers, we used the composite $(\text{La}_{0.8}\text{Sr}_{0.2})_{0.95}\text{MnO}_3$ /10Sc1CeSZ and single-phase perovskite $(\text{La}_{0.8}\text{Sr}_{0.2})_{0.95}\text{MnO}_3$ (LSM), which were sintered at 1100°C to prevent the formation of reaction layers with high resistance and to preserve high specific surface area. For small model SOFCs, the specific capacity recorded at a working temperature of 850°C reached 400 mW/cm^2 [8]. However, the electrochemical characteristics became much worse when large solid-electrolyte membranes were used [9].

This study is devoted to the development of a procedure for the preparation of SOFC MEAs by co-sintering of electrodes and investigation of their electrochemical characteristics.

¹ Presented at the III All-Russian Conference “Fuel Cells and Energy Units on Their Basis,” Chernogolovka, 2015.

METHODS AND STARTING MATERIALS

The MEA samples were prepared from membranes of Fuel Cell Materials (Unites States). The membranes made of the Hionic™ anion conductor had a square shape with rounded angles; the square side was 50 mm, and the membrane thickness was 150 μm. The cathode layers were made of highly disperse 10Sc1CeSZ powder (DKKK, Japan) and cation-deficient manganite ($\text{La}_{0.8}\text{Sr}_{0.2}\text{MnO}_3$ (LSM) synthesized by citrate technology. For optimization of the microstructure, we used channel black K-354 (Spektr-Khim, Russia). The composite anode layers were prepared using 10Sc1CeSZ and NiO powders (Sigma Aldrich). As a pore-forming agent in the anode current collector layer, rice starch was used (Beneo, Belgium).

The highly disperse single-phase LSM powder was synthesized by the citrate method [10, 11] from $\text{La}(\text{NO}_3)_3 \cdot 6\text{H}_2\text{O}$, $\text{Sr}(\text{NO}_3)_2$, $\text{Mn}(\text{CH}_3\text{COO})_2 \cdot 4\text{H}_2\text{O}$, and citric acid monohydrate. The final annealing after the synthesis was performed in air at 1100°C with storage for 5 h.

To prepare the composites of the mixture of the starting compounds, many-stage millings were performed in a Pulverisette 5 ball mill (Fritsch, Germany). The millings were carried out in a vessel of partially stabilized ZrO_2 using balls of the same material with a diameter of 3 and 10 mm; a medium for milling was a toluene–butanol–diethyladipinate mixture with a volume ratio of 70 : 30 : 2 with a diaminopropane addition (3 wt %), which served as a surfactant.

The pastes for screen printing were prepared using Heraeus V-006A organic binder (Germany). The powder to binder ratio was 1 : 0.4 and 1 : 0.5 in the functional and current-collecting anode layers, respectively, and 1 : 0.8 and 1 : 1 in the functional and current-collecting cathode layers, respectively. These ratios were optimized earlier [12]. The multistage mixings for homogenization and degassing were performed in an ARE-250 planetary mixer (Thinky, Japan). The electrode pastes were applied to the solid electrolyte membranes by screen printing using an Ekra Mat S45 tool (Ekra, Germany) through templates of A-Design production (Russia).

The XRD analysis of the starting materials was performed using a Siemens D-500-Braun X02-1787 diffractometer ($\text{CuK}_{\alpha 1}$ radiation, step 0.02°, 20° ≤ 2θ ≤ 90°) (Siemens, Germany). The morphology of the starting powders and the microstructure of the membranes of the solid electrolyte and electrode layers were studied using a LEO Supra 50VP scanning electron microscope (SEM) with a field emitting cathode equipped with an INCA Energy+ microanalysis system for X-ray fluorescence spectral microanalysis studies. Studies by high-resolution transmission electron microscopy were performed using a Jeol JEM-2100

microscope (Japan). For thermogravimetric studies of the pore-forming agents and the binder, a Setsys EVO 16/18 thermogravimetric analyzer (Setaram, France) was used.

The electrochemical characteristics of MEAs were studied using a TrueXessory-HT unit (FuelCon, Germany) and the gas-temperature stand for control over the working temperature of the flow and the composition of the oxidative and reductive gas mixtures. The hodographs of the impedance spectra were measured in the frequency range 0.1 Hz–1 MHz using an Autolab 302N potentiostat galvanostat with a FRA-32M2 module by the electrode four-contact method, which allows the resistance of current-carrying wire to be excluded.

RESULTS AND DISCUSSION

Membrane Electrode Assemblies

For higher efficiency of operation of SOFCs, both electrodes consisted of two layers that differed in the composition and microstructure. The (functional) layer adjacent to the supporting electrolyte was optimized for effective redox reactions. The aim of the outer (current-collecting) electrode layer is the distribution of the gas flows of reagents and reaction products and the decrease in the layer resistance to the electron current.

Cathodes. The structure and morphology of the synthesized LSM, which is the basis for SOFC cathodes, were studied by XRD analysis and scanning electron microscopy. The powder diffraction pattern and the SEM image are shown in Fig. 1. An analysis showed that the synthesized LSM is single-phase and has the structure of rhombohedral perovskite ($a = 0.5478(3)$ nm, $V = 0.1176$ nm³). The manganite powder consists of submicron-sized particles (0.1–0.8 μm) united into agglomerates with a size of up to 5 μm, due to which it can be used for the preparation of the current-collecting layer of the cathode electrode. The use of this powder in the functional layer of the electrode requires preliminary deagglomeration by grinding.

To prepare a current-collecting layer, we used pure LSM, which was not preliminarily ground in a planetary mill. The functional layer of the cathodes was prepared from a composite with a weight ratio of LSM : 10Sc1CeSZ = 60 : 40%. For optimization of the microstructure, 15 wt % channel black was introduced as a pore-forming agent in the composite. This choice of soot was dictated by the close particle sizes of the pore-forming agent and the oxide components (Figs. 1b and 2). This allows us to avoid the appearance of large pores in the cathode's functional layer and thus a decrease in the total length of the three-phase boundary between the electrode, the solid electrolyte, and the gas phase. To prepare a composite

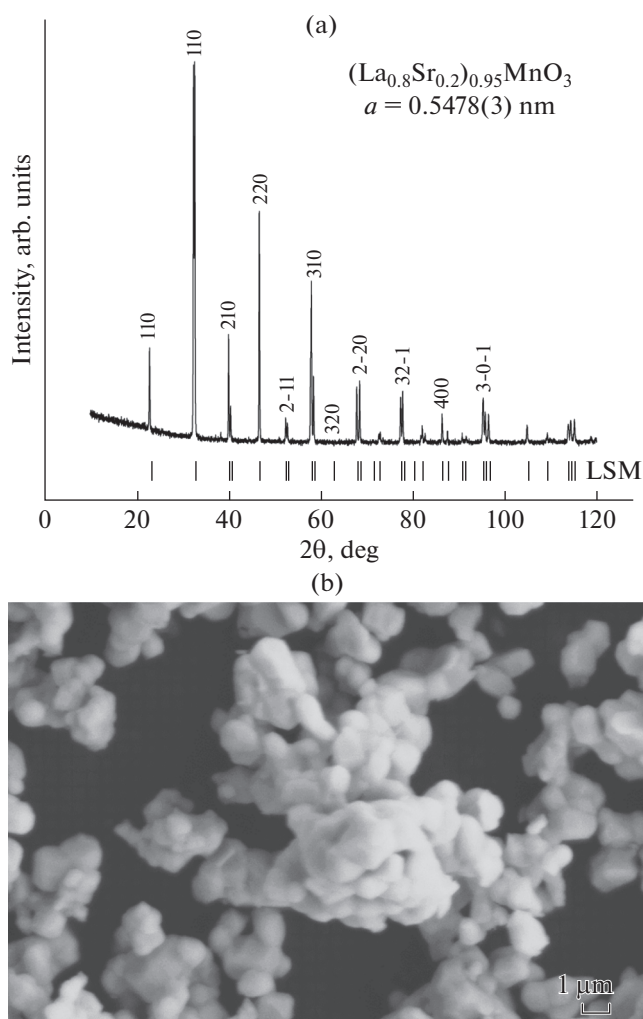


Fig. 1. (a) Powder diffraction pattern of LSM and (b) SEM image of the powder particles.

mixture, the starting powder samples of LSM, 10Sc1CeSZ, and channel black were subjected to preliminary co-grinding in a planetary mill followed by homogenization of the mixture in a biaxial mixer.

Anodes. The anode layers were prepared from 10Sc1CeSZ and NiO composites. The ratio of these phases in the functional and current-collecting layers of the anode was optimized earlier [13, 14] (40 : 60 and 60 : 40 wt %, respectively). The rice starch pore-forming agent (10 wt %) was introduced in the current-collecting layer.

Note that the starting nickel oxide nanopowder (Aldrich, <50 nm) is not suitable for use for the preparation of electrode pastes and requires preliminary preparation. As shown in [15], the particles of nanostructured NiO have a “core-shell” type structure (Fig. 3a). The amorphous shell of the particles has adsorbed water and superstoichiometric oxygen, which should be removed. For this reason, the nickel

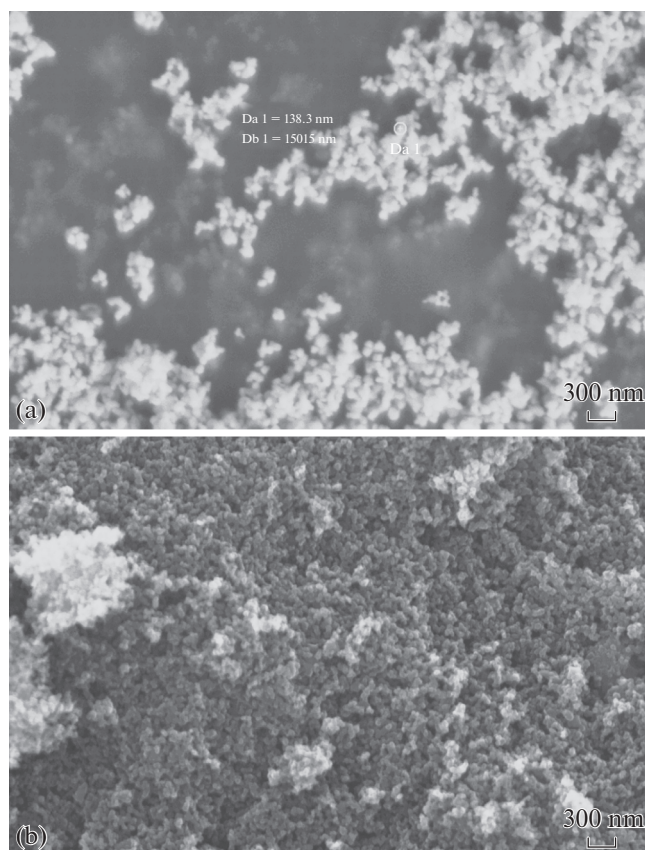


Fig. 2. SEM images of (a) 10Sc1CeSZ and (b) channel black powder.

oxide powder used in the functional and current-collecting layers of the anode was preliminarily annealed at 650 and 900°C, respectively.

The SEM image of the NiO powder after annealing at 650°C for 1 h is shown in Fig. 3b. After the thermal treatment, the nickel oxide particle size was 50–100 nm, which is comparable to the particle size of 10Sc1CeSZ powder (Fig. 2a). To prepare a composite mixture, the NiO and 10Sc1CeSZ samples were subjected to co-grinding followed by homogenization in a mixer.

To increase the gas permeability of the anode’s current-collecting layer, pore-forming agents are generally used, whose combustion forms a system of main pores in the electrode layer. Figure 4 shows the SEM images of rice and potato starch powders, which were considered for this purpose. The potato starch particles (Fig. 4b) have a wide pore size distribution; the individual particles have sizes of up to 70 μm, which considerably exceeds the thickness of the current-collecting layer. The rice starch particles have the shape of irregular polyhedra, whose average size is 3–5 μm. This size is well suitable for creating a developed system of main pores.

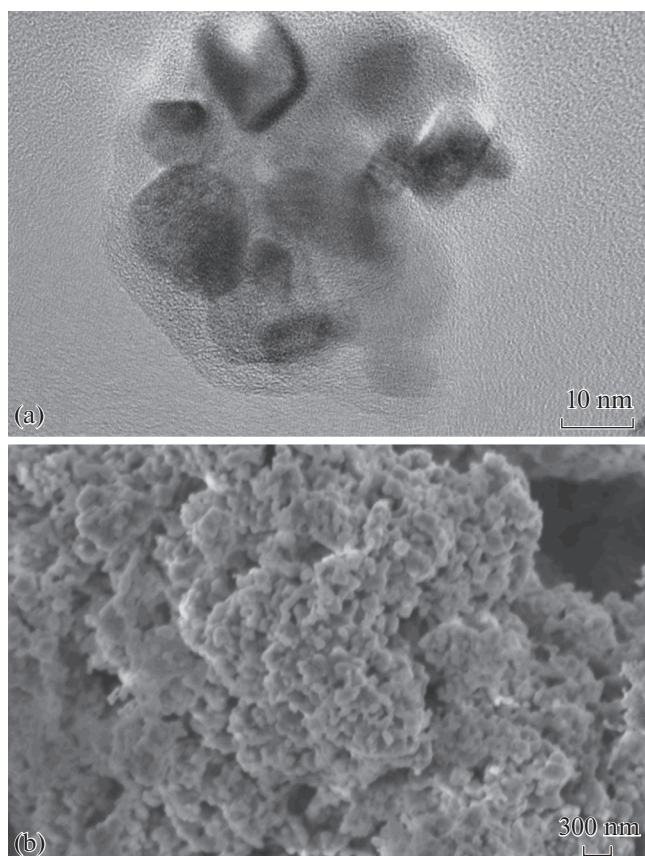


Fig. 3. (a) TEM image of the starting NiO and (b) SEM image of the NiO powder annealed at 650°C.

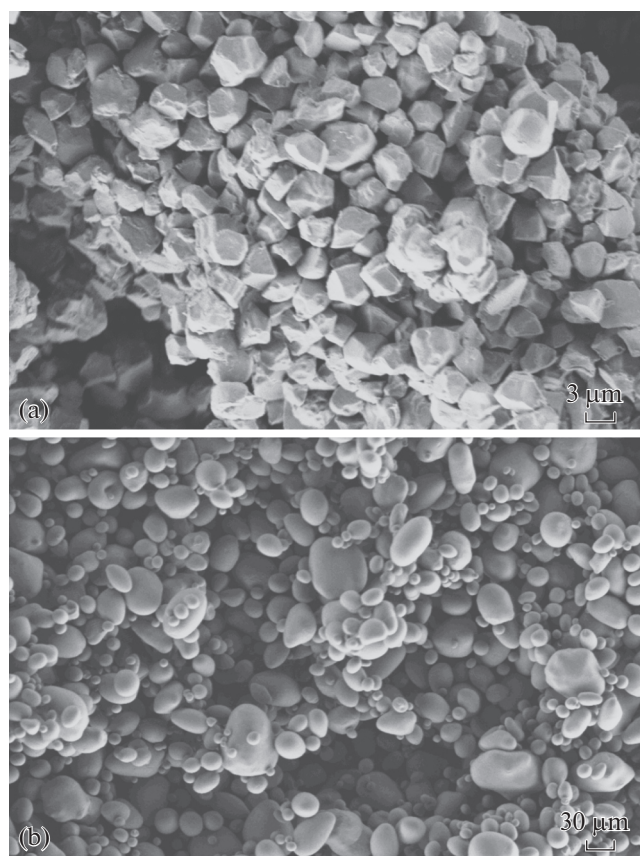


Fig. 4. SEM images of (a) rice and (b) potato starch powder.

To determine the optimum amount of rice starch to be introduced in the current-collecting layer of the node, a series of samples with 0, 5, 7.5, 10, 12.5, and 15 wt % starch were prepared [16]. The SEM images of the transverse section of the anode electrode with 0, 5, 10, and 15% starch are presented in Fig. 5.

According to the figures, the starting sample prepared without a pore-forming agent contains a developed pore system with a characteristic size of $\sim 1 \mu\text{m}$ (Fig. 5a). After the addition of 5 wt % rice starch (Fig. 5b), large pores of up to $\sim 5 \mu\text{m}$ appear along with small ones, but the large pores are not connected. An increase in the fraction of rice starch to 10 wt % (Fig. 5c) leads to the appearance of a connected developed system of main pores. As the starch content increases further to 15% (Fig. 5d), both the fraction of large pores and their average size increase, which can drastically deteriorate the mechanical and electroconducting properties of the current-collecting layer. For this reason, the optimum mass content of rice starch in the current-collecting layer of the anode electrode of SOFCs is $\sim 10 \text{ wt } \%$. The mixture of NiO, 10Sc1CeSZ, and starch powders was subjected to co-grinding in a planetary mill followed by homogenization in a biaxial mixer.

Choice of the Thermal Treatment Mode

For optimization of the heating stage when choosing the high-temperature annealing mode of MEA, rice starch, channel black, and organic binder were studied by thermogravimetric analysis. The measurements were performed in air atmosphere at a heating rate of 2 K/min. Figure 6 presents the temperature dependences of the mass and its first derivative. The complete combustion of rice starch requires a temperature not lower than 480°C. We can isolate three stages of mass loss. The insignificant change in the mass on heating to 200°C is possibly explained by the loss of sorbed water. The starch components actively burnt out at temperatures from 250 to 300°C and less actively in the range from 300 to 480°C. Channel black completely burns out on heating to 720°C. The mass loss starts at $\sim 375^\circ\text{C}$; then the process accelerates up to 600°C.

Figure 7 shows the thermogravimetric data on combustion of the HeraeusV006-A binder. The mass loss mainly occurs in the temperature range 100–250°C. The remaining 10% burn out at temperatures of up to 400°C.

The optimum heating mode during the high-temperature annealing of SOFC MEAs was determined

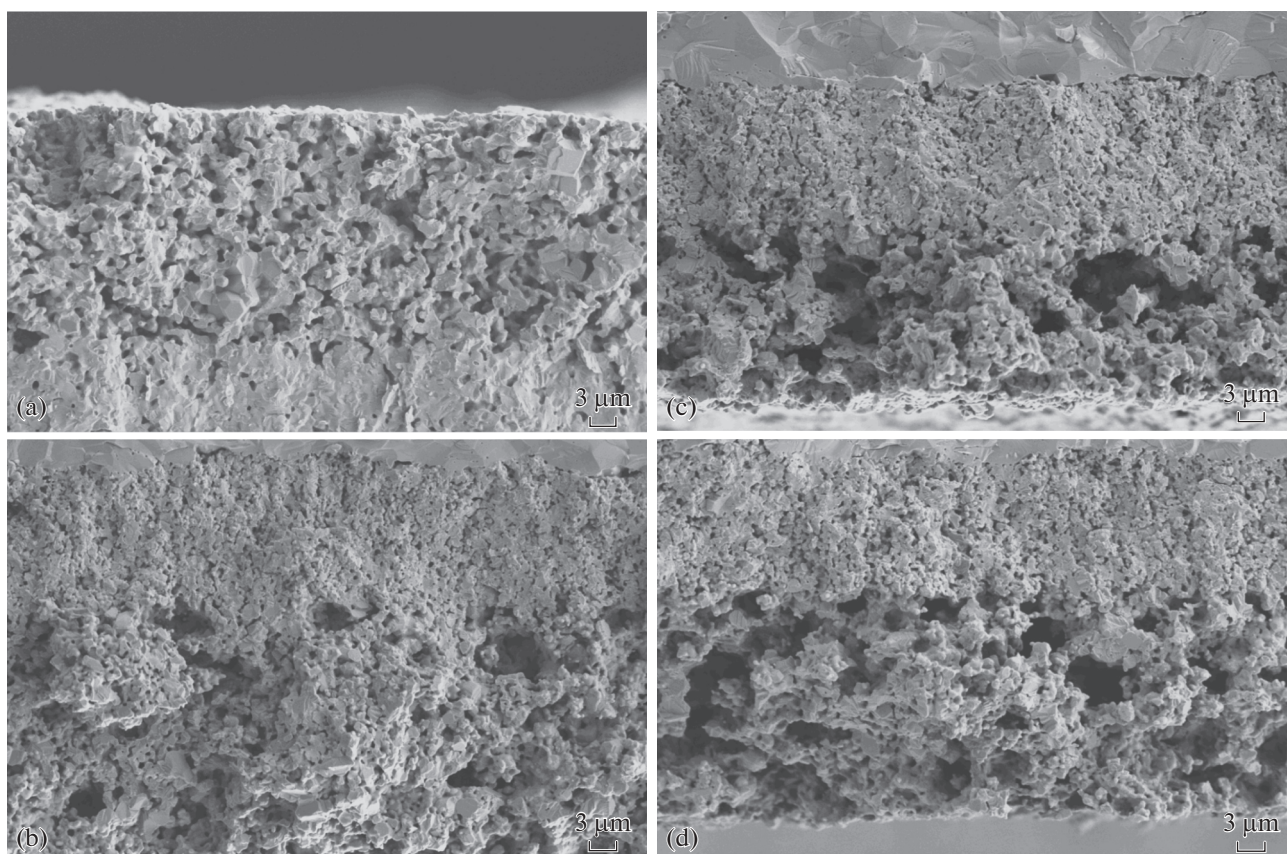


Fig. 5. SEM images of the samples with different rice starch contents in the current-collecting anode layer: (a) 0, (b) 5, (c) 10, and (d) 15 wt %.

based on the results of the thermogravimetric analysis. The first stage of heating to 250°C was performed at a high rate for 1 h because the volatile components of the Heraeus V-006A binder were preliminarily removed during the drying in air at 130°C after the deposition of each of the four electrode layers. To remove the heavy organic binder and the pore-forming agent powders (rice starch and channel black), the heating to 750°C was performed at a rate of 100 K/h.

The maximum temperature of thermal treatment is the most important parameter of high-temperature annealing during the co-sintering of electrodes. If sequential sintering of electrodes is used, the anode annealing temperature is generally higher than 1300°C, which allows the formation of well-sintered cermet that provides sufficient density of the three-phase boundary combined with its good stability under the working conditions of SOFCs. The preliminary studies showed that when the temperature of formation of the anode electrode decreases below 1170°C, the electrochemical characteristics of SOFCs quickly degrade, which is possibly explained by the low density of the formed electrode layers and hence the worse electroconductive properties and possibly worse local contacts. The temperature of formation of

cathode layers is considerably limited by the possibility of chemical interaction of the cathode material with the material of the solid-electrolyte membrane and should not be exceed 1150°C. The use of cation-deficient lanthanum-strontium manganite allows us to markedly suppress this interaction; however, according to Fig. 8, an increase in the sintering temperature above 1150°C leads to an appreciable decrease in the porosity of the composite functional layer of the cathode. Therefore, pore-forming agents should be introduced in order to increase the temperature of formation of cathode layers.

According to Fig. 9, the use of 15 wt % channel black as a pore-forming agent in the composite of the functional layer of the cathode allows a considerable increase in the fraction of pores during the sintering up to 1170°C. This temperature was chosen as the optimum temperature of high-temperature annealing for co-sintering of SOFC electrodes.

The optimum conditions of high-temperature annealing of SOFC MEAs were chosen based on the thermogravimetric analysis of the pore-forming agents and binder and the results of temperature optimization of final annealing. The time dependence of the annealing temperature is shown in Fig. 10.

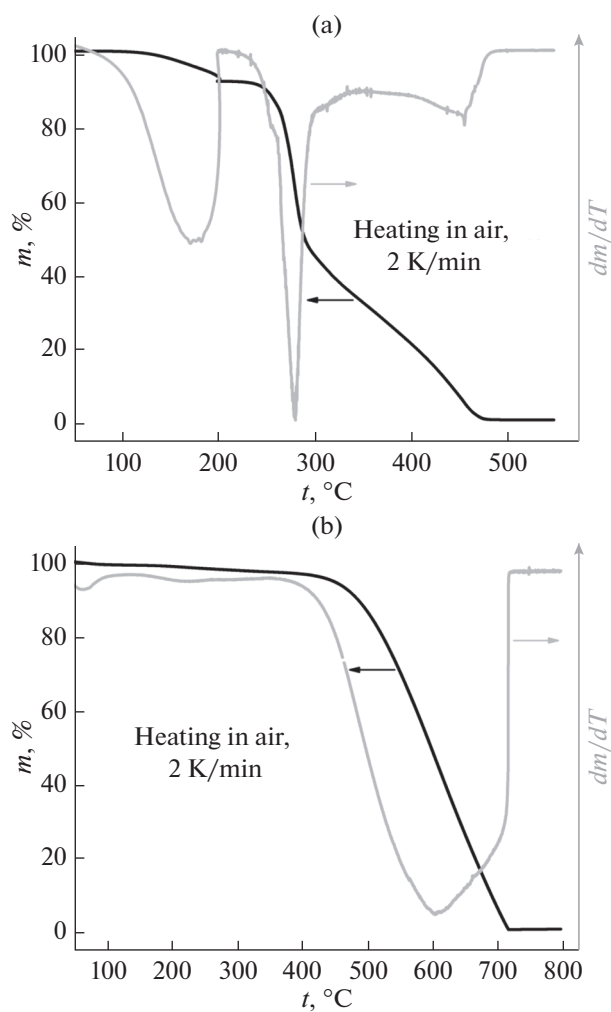


Fig. 6. Results of the thermogravimetric analysis of (a) rice starch and (b) channel black.

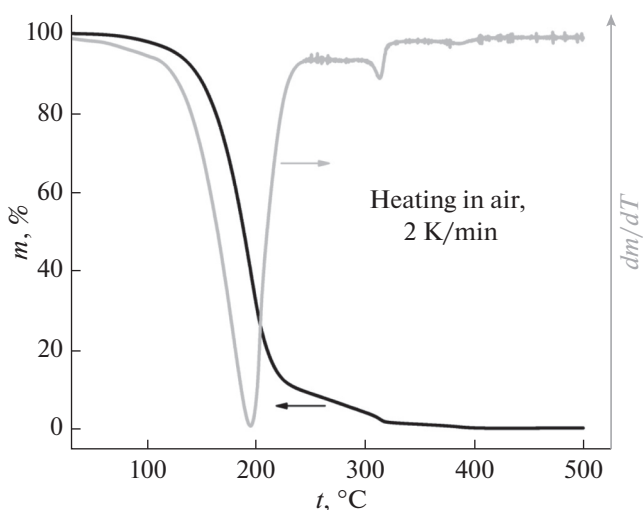


Fig. 7. Results of the thermogravimetric analysis of the Heraeus V006A binder.

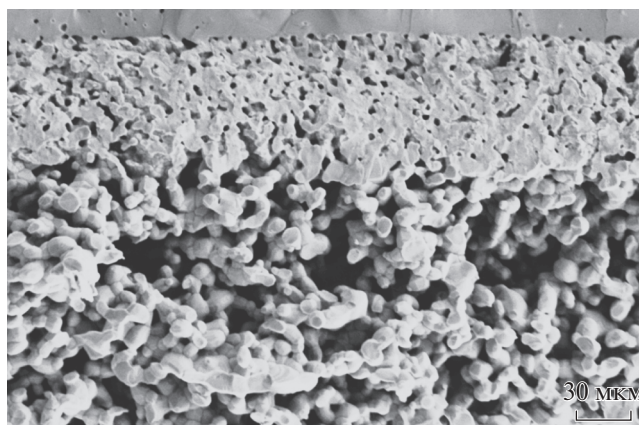


Fig. 8. SEM image of the cathode electrode of SOFC prepared without using any pore-forming agents and sintered at 1155°C.

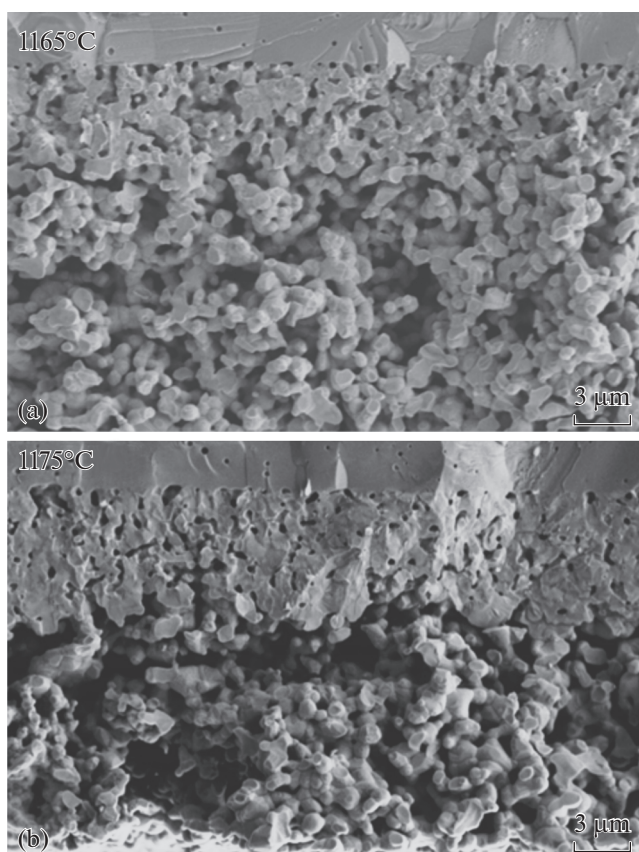


Fig. 9. SEM images of the cathode electrode of SOFC prepared using pore-forming agents and sintered at (a) 1165 and (b) 1175°C.

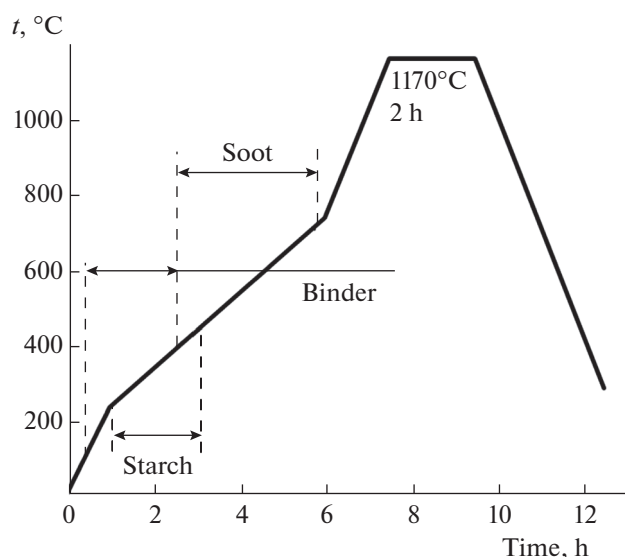


Fig. 10. High-temperature annealing mode of membrane-electrode assemblies for combined formation of electrodes.

Microstructural and Electrochemical Characteristics of MEAs

After optimization of the morphology of the starting materials, the composition of the electrode composites, and the thermal treatment conditions, a series of membrane-electrode assemblies of SOFCs were

prepared by co-sintering of electrodes. The photographs of the SOFC MEA samples are given in Fig. 11.

The transverse section of the model samples was studied by scanning electron microscopy (Fig. 12). It can be seen that the layers are uniform in thickness. The thickness of the functional cathode layer is $\sim 10 \mu\text{m}$, and that of the current-collecting layer is $\sim 20 \mu\text{m}$. The anode electrode consists of the functional and current-collecting layers each with a thickness of $\sim 20 \mu\text{m}$.

Figure 13 shows the SEM images of the individual cathode and anode obtained at larger magnification. Both the electrode layers and the phase boundaries are well sintered. The current-collecting layers of electrodes have a developed system of main pores with a size of more than $3 \mu\text{m}$, and the functional layers are formed from submicron particles. Note that the use of channel black as a pore-forming agent during the preparation of the cathode's functional layer of SOFCs allowed us to avoid a considerable increase in the mean particle size of lanthanum-strontium manganite and $10\text{Sc}1\text{CeSZ}$, but the pore volume may be insufficient.

The electrochemical characteristics of the membrane-electrode assemblies prepared by co-sintering of electrodes were studied at 850°C . The fuel mixture consisted of hydrogen and nitrogen at a partial pressure of 0.5 atm. As the oxidative mixture, we used mixtures of oxygen and nitrogen with a partial oxygen pressure of 0.21 atm (artificial air) and 0.5 atm. The

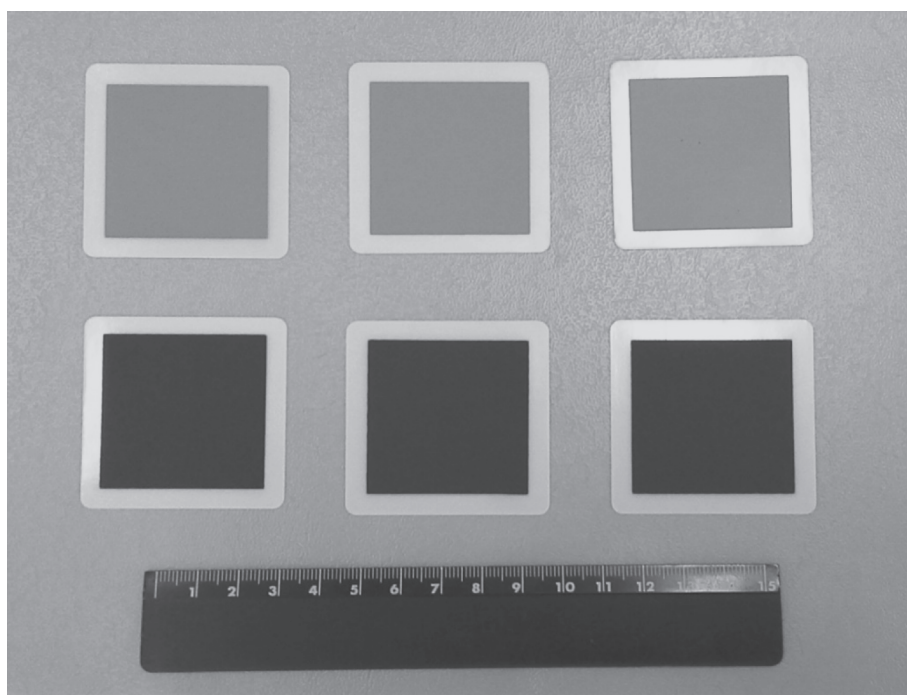


Fig. 11. Photographs of the membrane-electrode assemblies of SOFC prepared by co-sintering of electrodes.

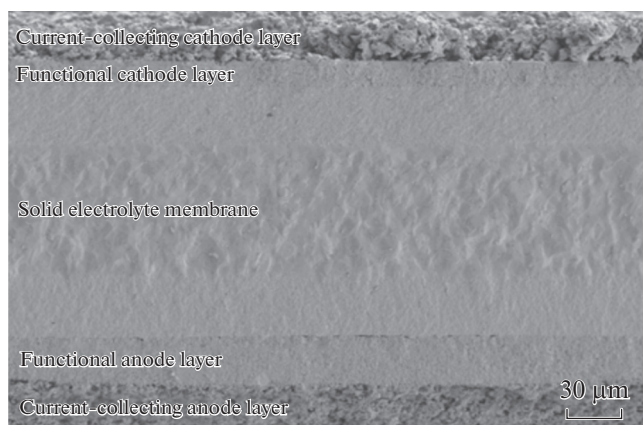


Fig. 12. SEM image of the transverse section of SOFC MEA prepared by co-sintering of electrodes.

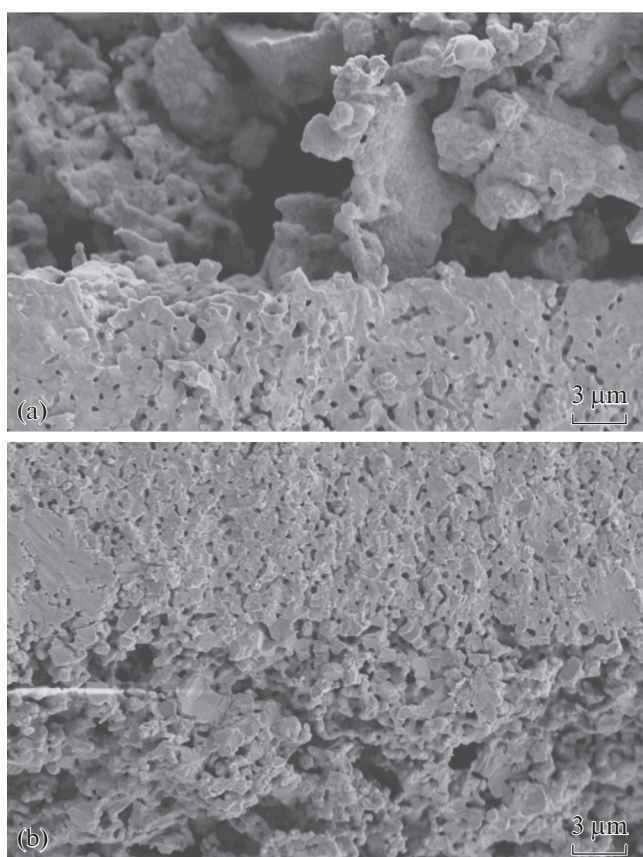


Fig. 13. SEM image of the (a) cathode and (b) anode electrodes of the SOFC MEA prepared by co-sintering of electrodes.

voltage-current and capacity characteristics of SOFC MEAs are shown in Fig. 14. When air was used as an oxidant, the maximum capacity recorded on MEA was above 3.6 W (specific capacity 225 mW/cm²). Note that this value of recorded capacity was achieved at a voltage of 0.7 V; the resistance of the supply leads

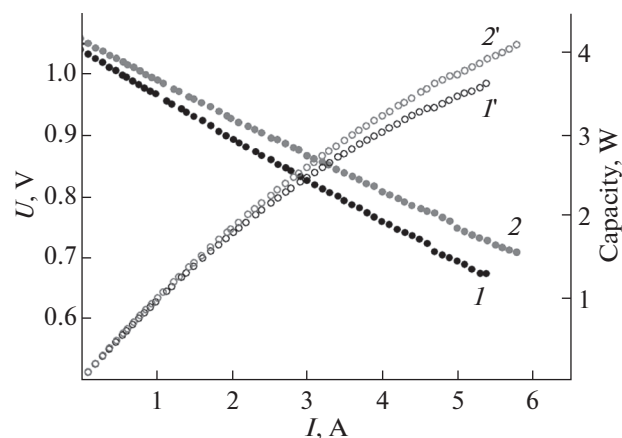


Fig. 14. Voltammetric and capacity characteristics of SOFC MEA prepared by co-sintering of electrodes. (*I, I'*) $p(\text{H}_2) = 0.5$ bar, $p(\text{O}_2) = 0.21$ bar; (*2, 2'*) $p(\text{H}_2) = 0.5$ bar, $p(\text{O}_2) = 0.21$ bar.

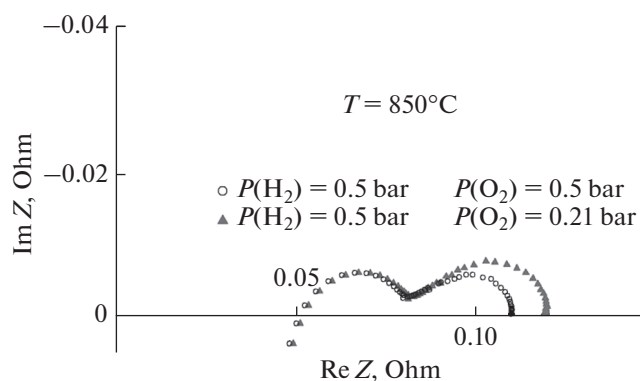


Fig. 15. Impedance spectrum hodographs of SOFC MEA with electrodes with an area of 4 × 4 cm².

and the specifics of the measuring station prevented the capacity from passing through a maximum. When richer oxidation mixtures were used, the recorded capacity exceeded 4.2 W (260 mW/cm²). The appreciable improvement of the electrochemical characteristics of at increased partial oxygen pressure is probably explained by diffusion hindrances on the fuel cell cathode.

To determine the components of the total resistance of SOFC MEAs under the same working conditions, we studied the hodographs of the impedance spectrum. Some of the results are shown in Fig. 15. It can be seen that the ohmic part of the impedance spectrum is ~0.05 Ohm (0.8 Ohm cm²), and the polarization part is 0.06 Ohm (1.0 Ohm cm²) when a rich oxidative mixture was used and ~0.07 Ohm (1.1 Ohm cm²) for the artificial air. Note that the change in the partial oxygen pressure has a significant effect exactly on the low-frequency part of the hodograph, generally

related to the diffusion contribution to the polarization resistance. This is confirmed by the previous assumption about the diffusion hindrances on the SOFC cathode.

CONCLUSIONS

The results of the development of a procedure for the preparation of SOFC MEAs by co-sintering of electrodes were presented. This technology allows the compensation of mechanical stresses arising in a solid-electrolyte membrane during high-temperature annealing. Our electrochemical studies showed that the maximum specific capacity recorded on MEAs is 225 mW/cm² at a working temperature of 850°C and a cell voltage of 0.7 V. A study of the dependence of the impedance spectrum hodograph on the partial oxygen pressure points to gas hindrances on the cathodes possibly associated with the insufficient porosity of the functional layer. Further studies will deal with optimization of the microstructure of this layer to increase the density and capacity recorded on SOFC MEAs.

ACKNOWLEDGMENTS

This study was financially supported by the Ministry of Education and Science of the Russian Federation (Studies and Developments on Priorities of Science and Technology federal program, unique identifier of the agreement RFMEFI61014X0007) and the Russian Foundation for Basic Research (project no. 13-03-12408).

REFERENCES

1. Ivers-Tiffée, E., Weber, A., and Herbstritt, D., *J. Eur. Ceram. Soc.*, 2001, vol. 21, p. 1805.
2. Selimovic, A., Kemm, M., Torisson, T., and Assadi, M., *J. Power Sources*, 2005, vol. 145, p. 463.
3. Nakajo, A., Stiller, C., Harkegard, G., and Bolland, O., *J. Power Sources*, 2006, vol. 148, p. 287.
4. Anam, K. and Lin, C.K., *Appl. Mech. Mater.*, 2014, vol. 493, p. 331.
5. Bouhala, L., Belouettar, S., Makradi, A., and Remond, Y., *Mater. Des.*, 2010, vol. 31, p. 1033.
6. Muller, A.C., Herbstritt, D., and Ivers-Tiffée, E., *Solid State Ionics*, 2002, vol. 152, p. 537.
7. Mucke, R., Menzler, M.H., Buchkremer, H.P., and Stover, D., *J. Am. Ceram. Soc.*, vol. 92, p. 95.
8. Burmistrov, I., Agarkov, D., Bredikhin, S., Nepochatov, Yu., Tiunova, O., and Zadorozhnaya, O., *ECS Trans.*, 2013, vol. 57, p. 917.
9. Tiunova, O.V., Zadorozhnaya, O.Yu., Nepochatov, Yu.K., Burmistrov, I.N., Kuritsina, I.E., and Bredikhin, S.I., *Russ. J. Electrochem.*, 2014, vol. 50, p. 719.
10. Kolotygin, V.A., Tsipis, E.V., Ivanov, A.I., Fedotov, Y.A., Burmistrov, I.N., Agarkov, D.A., Sinitsyn, V.V., Bredikhin, S.I., and Kharton, V.V., *J. Solid State Electrochem.*, 2012, vol. 16, p. 2335.
11. Ivanov, A.I., Agarkov, D.A., Burmistrov, I.N., Kudrenko, E.A., Bredikhin, S.I., and Kharton, V.V., *Russ. J. Electrochem.*, 2014, vol. 50, p. 730.
12. Agarkov, D.A., *M.Sc. Dissertation*, Chernogolovka: Inst. of Solid State Physics, Russ. Acad. Sci., 2013.
13. Bredikhin, I., Sinitsyn, V., Aronin, A., Kutitsina, I., and Bredikhin, S., *ECS Trans.*, 2007, vol. 7, p. 1541.
14. Bredikhin, I., Bredikhin, S., and Kveder, V., *ECS Trans.*, 2009, vol. 25, p. 1967.
15. Burmistrov, I.N., Agarkov, D.A., Tartakovskii, I.I., Kharton, V.V., and Bredikhin, S.I., *ECS Trans.*, 2015, vol. 68, p. 1265.
16. Zaitseva, D.V., Agarkov, D.A., Burmistrov, I.N., and Bredikhin, S.I., Abstracts of Papers, *Vserossiiskaya konferentsiya s mezhdunarodnym uchastiem "Toplivnye elementy i energoustanovki na ikh osnove"* (All-Russian Conf. with Foreign Participants "Fuel Cells and Energy Units on their Basis), Chernogolovka, 2015, p. 128.

Translated by L. Smolina

SPELL: 1. ok